Astron. Astrophys. 335, 522–532 (1998)

ASTRONOMY AND ASTROPHYSICS

ISO observations of candidate young brown dwarfs⋆

F. Comerón[1], G.H. Rieke[2], P. Claes[3], J. Torra[4], and R.J. Laureijs[3]

[1] European Southern Observatory, Karl-Schwarzschild-Strasse 2, D-85748 Garching bei München, Germany
[2] Steward Observatory, University of Arizona, Tucson, AZ 85721, USA
[3] Infrared Space Observatory, European Space Agency, Villafranca del Castillo Satellite Tracking Station, P.O. Box 50727, E-28080 Madrid, Spain
[4] Departament d'Astronomia i Meteorologia, Universitat de Barcelona, Av. Diagonal, 647, E-08028 Barcelona, Spain

Received 24 July 1997 / Accepted 22 April 1998

Abstract. ISOCAM measurements or upper limits for low mass members of the ρ Ophiuchi embedded cluster extend the sampling of the spectral energy distributions already obtained from the ground towards longer wavelengths, where emission by circumstellar material is significant. Good fits to the combined (ground-based + ISOCAM) photometry are obtained with theoretical models of pre-main sequence evolution, complemented with models of the spectrum of circumstellar emission, synthetic spectra of cold atmospheres, and an extinction law. The most important physical parameters of the targets, such as mass and luminosity, can be estimated with more confidence than with ground-based data alone, thanks to the much more robust reconstruction of the intrinsic spectral energy distribution made possible by the new ISOCAM data.

An object-by-object discussion, based on both published and new material, shows that estimates of the source temperatures from fitting of the photometry agree closely with spectroscopy for all seven sources where both techniques have been applied. The agreement between the new fits and those based on groundbased photometry alone is also reasonably good. Three of the sources are very likely to be young brown dwarfs, five are transitional, and three appear to be low mass stars.

Key words: stars: formation – stars: low mass, brown dwarfs – infrared: stars

1. Introduction

Intense theoretical and observational efforts have been devoted recently to identification of brown dwarfs and to study of their properties. This effort is justified by their intrinsic interest as transition objects between stars and planets, but also by their role in a wide range of astrophysical problems, such as their contribution to the dark matter content of galactic disks, or the insights they provide to the processes of accretion and fragmentation leading to star formation. Moreover, they can test models of pre-main sequence evolution at very low masses and probe the complex chemistry of cool photospheres. Until recently the search for these objects had produced only probable candidates (see summary in Trimble 1995). However, the situation has changed dramatically in the last two years, with the detection of several objects with clearly substellar and even planetary masses (Rebolo 1998).

The discovery of *bona-fide* brown dwarfs elsewhere heightens the interest in searches for such objects in embedded clusters. In addition to the important observational advantage of relatively high luminosity and temperature, these sources sample a region of the temperature-surface-gravity diagram already abandoned by the more evolved brown dwarfs. Their potential detectability in significant numbers enables derivation of the shape of the low mass and substellar initial mass function, which is not possible at present with the evolved brown dwarfs. However, the observational distinction between massive brown dwarfs and very low mass stars is subtle at the ages of embedded clusters, and furthermore it can be masked by age effects and by circumstellar material.

The ρ Ophiuchi clouds contain one of the most nearby and most thoroughly studied populations of young stellar objects. Surveys of the area have been conducted at a variety of wavelengths (Barsony et al. 1989; Rieke et al. 1989; Wilking et al. 1989; Leous et al. 1991; André et al. 1992; Bouvier & Appenzeller 1992; Greene & Young 1992; Mezger et al. 1992; Comerón et al. 1993; André & Montmerle 1994; Greene et al. 1994; Casanova et al. 1995; Greene & Meyer 1995; Strom et al. 1995; Greene & Lada 1996; Barsony et al. 1997; Kenyon et al. 1998). Photometric and spectroscopic surveys in the near infrared have provided insights to the stellar mass function and the evolutionary status of the aggregate.

Nevertheless, some uncertainty remains in the classification of the faintest embedded sources, such as the relatively blue objects which are very likely substellar (Rieke & Rieke 1990, Comerón et al. 1993, Williams et al. 1995). High quality spectroscopy is not feasible for these sources, and photometric techniques are subject to potentially distorting effects from

Send offprint requests to: F. Comerón

⋆ Based on observations with ISO, an ESA project with instruments funded by ESA Member States (especially the PI countries: France, Germany, the Netherlands and the United Kingdom) with the participation of ISAS and NASA.

Table 1. Candidate brown dwarfs from JHK photometry

2320.8-1721
2321.6-1918
2322.8-1233
2331.1-1952
2349.8-2601
2404.5-2152
2408.6-2229

circumstellar material and line-of-sight extinction. To account for these factors more accurately, it is necessary to have a wide wavelength coverage, as has been made possible by the imaging camera ISOCAM on the Infrared Space Observatory (ISO). In this paper, we present and discuss the results of ISOCAM observations of some of the candidate brown dwarfs in ρ Ophiuchi. Some of the fields selected for our ISOCAM observations also contain low mass stars, whose characteristics we analyze together with those of the candidate brown dwarfs. In addition, we present recent follow-up observations in the visible and near infrared of one of the fields imaged by ISO.

Our source selection criteria and observations are described in Sect. 2. Sect. 3 summarizes our method of analysis. The results, including an object-by-object discussion, are presented in Sect. 4. Our conclusions are summarized in Sect. 5. Technical details of the ISOCAM data analysis are given in Appendix A.

2. Observations

2.1. Source selection

Our sample was drawn from the analysis of ρ Ophiuchi presented by Comerón et al. 1993 (hereafter CRBR), who used an early version of the method described in Sect. 3 to identify possible brown dwarfs. Refinements of the analysis method and the incorporation of new theoretical isochrones (Burrows et al. 1993; D'Antona & Mazzitelli 1994) essentially confirmed our previous results, which were also independently supported by K-band spectroscopy (Williams et al. 1995). We selected as ISO targets brown dwarf candidates with weak or no infrared excess in the model fit. Fits to the ISOCAM fluxes of objects with strong infrared excess would be dominated by the emission of a circumstellar disk or envelope, and a comparison to theoretical isochrones (which ultimately would yield the mass of the central object) would therefore be very indirect. An exception was made for source 2320.8-1721, since its 2 μm spectrum supports its substellar nature. The list of our primary ISO targets is given in Table 1. The denomination of sources is the same as in CRBR; namely, the first set of digits correspond to the offset in minutes and seconds of right ascension from 16h, and the second set, to the offset in minutes and seconds of declination from -24^0 (1950.0 coordinates)

The centers of the ISOCAM frames were chosen to include other nearby objects, in most cases low mass stars. This enabled us to apply our method on a well sampled spectral energy distribution for objects over a fairly large range of masses. The results help us assess the validity of the method for the study of the statistical properties of larger samples of objects, often with only JHK photometry available (Comerón et al. 1996)

Table 2. Log of ISOCAM observations

Field	Objects included	Filter and date of observation
Oph1	2317.3-1925	SW1, 17 March 1996
	2320.0-1915	LW1, 19 March 1996
	2321.6-1918	LW2, 10 August 1996
		LW4, 18 August 1997
Oph2	2317.5-1729	SW1, 9 August 1997
	2319.8-1617	LW1, 14 March 1996
	2320.8-1708	LW2, 7 September 1996
	2320.8-1721	LW4, 18 March 1996
	2321.1-1715	
	2321.1-1754	
	2321.2-1719	
	2322.6-1802	
	2323.8-1640	
Oph3	2322.8-1233	SW1, 18 August 1997
		LW1, 9 August 1997
		LW2, 18 August 1997
		LW4, 18 March 1996
Oph4	2331.1-1952	SW1, 18 March 1996
		LW1, 18 March 1996
		LW2, 18 March 1996
		LW4, 17 March 1996
Oph5	2349.8-2601	LW1, 18 March 1996
	2351.8-2553	LW4, 18 March 1996
Oph6	2404.5-2152	SW1, 18 March 1996
	2408.6-2229	LW2, 18 March 1996
		LW4, 18 March 1996

2.2. ISOCAM observations

Measurements were made in four ISOCAM bands. SW1 ($\lambda_{eff} = 3.6$ μm, $\lambda/\Delta\lambda = 3$) overlaps with the groundbased L' window and provides a direct comparison with the groundbased photometry. LW1 ($\lambda_{eff} = 4.5$ μm, $\lambda/\Delta\lambda = 5$) and LW4 ($\lambda_{eff} = 6.0$ μm, $\lambda/\Delta\lambda = 6$) should provide accurate photometry beyond the wavelengths accessible from the ground. LW2 ($\lambda_{eff} = 6.75$ μm, $\lambda/\Delta\lambda = 2$) was also used despite the reduced accuracy due to its wide bandpass, because of the potentially higher sensitivity. However, since this filter includes several interstellar emission features (Sellgren et al. 1985, Boulanger et al. 1988), the signal to noise in this band was not significantly better than with LW1 or LW4, and we will not include the LW2 results in our discussion.

The ISOCAM observations were obtained between March 1996 and August 1997. The log of observations is given in Table 2. Technical details on the instrumental setup and the exposure times, as well as the data reduction procedures, are given in Appendix A. Aperture photometry was performed on the flux-calibrated images and transformed to magnitudes. Zero-

magnitude fluxes, f_λ^0, at the central wavelengths of the ISOCAM filters were derived by linearly interpolating the function $f_\lambda^0 \lambda^{-\alpha}$, determining f_λ^0 and α from the zero-magnitude fluxes between neighboring positions tabulated by Engelke 1992. The derived values are close to the exponent $\alpha = 2$ corresponding to Rayleigh-Jeans behavior. The flux-to-magnitude transformations are thus:

$$m_{\rm SW1} = 13.70 - 2.5 \log f_{\rm SW1}[{\rm mJy}] \qquad (1a)$$

$$m_{\rm LW1} = 13.20 - 2.5 \log f_{\rm LW1}[{\rm mJy}] \qquad (1b)$$

$$m_{\rm LW4} = 12.47 - 2.5 \log f_{\rm LW4}[{\rm mJy}] \qquad (1c)$$

The magnitude measurements of the observed sources, combining ground-based and ISO results, are presented in Table 3. Some of the sources of field Oph2 listed in Table 2 have been excluded: 2318.9-1740, 2321.1-1754, and 2322.6-1802 are too bright and extended, and 2321.1-1715 and 2321.2-1719 cannot be distinguished from 2320.8-1721 at the resolution available. The ISOCAM magnitudes quoted for the latter source may therefore contain some contribution from the two fainter companions although, judging from their fainter magnitudes at bands short of L', we consider it unlikely that this contribution is significant. Magnitude uncertainties for ground-based observations are from CRBR. For ISO observations, the uncertainties were estimated by comparing measurements with different apertures and background reference regions. Lower limits for the ISO magnitudes correspond to 3σ over the local average background noise level.

2.3. New ground-based observations

The approximate area of field Oph2 was imaged in April 1997 in JHK using the IRAC2 infrared camera at the ESO-MPI 2.2 m telescope, as well as in the R and I bands using the ESO New Technology Telescope (NTT). A mosaic showing images of this field in R, I, J, K, LW1, and LW4 has been presented elsewhere (Comerón et al. 1997). The R and I photometry is listed in Table 4.

Table 4. R and I photometry of sources in the field Oph2

Object	R	I
2317.5-1729	> 25.7	23.29 ± 0.1
2320.8-1708	25.08 ± 0.2	22.09 ± 0.1
2320.8-1721	24.41 ± 0.2	21.44 ± 0.1

3. Analysis

3.1. Outline of the procedure

A detailed description of our analysis method applied to ground-based observations of embedded clusters has been published elsewhere (CRBR; Comerón et al. 1996), so we will only give an overview. Our goal is to determine the intrinsic properties of a young stellar object, possibly surrounded by a circumstellar disk or envelope, and embedded in a heavily obscuring molecular cloud. Foreground extinction decreases and reddens the observed fluxes. The circumstellar material tends to add primarily to the longer wavelength output, either by thermally reprocessing the shorter wavelength luminosity of the object, or through emission of the viscously heated material accreted onto the di sk.

In color-magnitude and color-color diagrams, therefore, the reddening vectors due to extinction and circumstellar excess are well separated. In the commonly used $(J-H)$, $(H-K)$ diagram, the T Tauri star locus can be explained by models of emission and reprocessing of radiation in circumstellar disks and envelopes (Adams et al. 1987; Lada & Adams 1992; Meyer et al. 1997; Calvet et al. 1997) and is easily distinguished from the effects of reddening (Strom et al. 1989). It is therefore possible in principle to derive the intrinsic properties of embedded objects by moving the observational data points in a multidimensional magnitude-color-color... diagram along the reddening and circumstellar excess vectors, until they fall on the locus defined by models of pre-main sequence evolution. The behavior of an embedded object is basically controlled by four parameters: luminosity, temperature, infrared excess, and foreground extinction (the distance can be usually considered as known and we have taken it to be 160 pc for ρ Oph). Therefore, to achieve a well constrained fit it is necessary to have measures in at least four bands, although three bands can suffice if one uses the theoretical isochrones and an assumed age to give a relation between luminosity and temperature. In practice, however, uncertainties in photometric measurements and possible deviations of real objects from the models used for the fits make it desirable to have a wide wavelength coverage in as many bands as possible to constrain the fits reliably. Our ISOCAM measurements provide an important advance in this regard.

3.2. Theoretical isochrones

The choice of the set of pre-main sequence evolutionary tracks is clearly an important aspect of the fit. In studies of emerged clusters, it is usually possible to place the object on a temperature-luminosity diagram, and then to estimate the mass and the age by overlaying the evolutionary tracks on the same diagram. However, mass estimates for embedded cluster members rely more strongly on the adopted evolutionary tracks, since in the procedure outlined above it is not possible to derive the temperature and luminosity independently of them.

Several recent sets of isochrones exist in the literature covering the mass range expected for our objects (Burrows et al. 1993, 1997; D'Antona & Mazzitelli 1994; Baraffe et al. 1997). A critical discussion of the different sets of isochrones from an observational point of view has been presented by Luhman 1998 and Luhman & Rieke 1998, who have examined the ability of existing models to reproduce the coevality of open cluster members, to provide well-behaved mass functions, and to fit

Table 3. Ground-based plus ISOCAM infrared photometry of the observed sources

Object	J	H	K	L'	SW1	LW1	LW4	N
2317.3-1925	14.87 ± 0.1	13.17 ± 0.1	12.04 ± 0.1	11.6 ± 0.2		10.10 ± 0.2	9.07 ± 0.2	
2317.5-1729	16.5 ± 0.2	13.85 ± 0.1	11.8 ± 0.1	10.0 ± 0.1	9.61 ± 0.1	9.92 ± 0.2		
2320.0-1915	12.56 ± 0.1	11.52 ± 0.1	10.89 ± 0.1	10.2 ± 0.1	9.76 ± 0.1	9.74 ± 0.1	9.44 ± 0.4	
2320.8-1708	15.80 ± 0.1	13.57 ± 0.1	12.23 ± 0.1	11.4 ± 0.2	11.03 ± 0.2	10.48 ± 0.2	10.16 ± 0.5	
2320.8-1721	16.36 ± 0.1	14.82 ± 0.1	13.55 ± 0.1	12.07 ± 0.2	12.17 ± 0.2	11.45 ± 0.2	10.31 ± 0.2	8.7 ± 0.4
2321.6-1918	19.2 ± 0.4	16.25 ± 0.1	13.85 ± 0.1	12.18 ± 0.2	> 11.6	12.16 ± 0.6	> 10.5	
2322.8-1233	>19.2	17.14 ± 0.1	14.88 ± 0.1	13.4 ± 0.2	> 12.9	> 13.5	>10.8	
2331.1-1952	16.66 ± 0.2	14.46 ± 0.1	13.19 ± 0.1	12.5 ± 0.4	12.37 ± 0.2	11.90 ± 0.4	10.86 ± 0.6	
2349.8-2601	15.4 ± 0.2	14.7 ± 0.2	14.2 ± 0.2			12.25 ± 0.3	>11.5	
2351.8-2553	>18.5	16.74 ± 0.1	12.98 ± 0.1	11.4 ± 0.1		9.80 ± 0.1	8.67 ± 0.2	
2404.5-2152	16.84 ± 0.1	14.63 ± 0.1	12.97 ± 0.1	11.8 ± 0.4	> 12.4		10.86 ± 0.4	
2408.6-2229	16.8 ± 0.1	15.1 ± 0.1	14.2 ± 0.1	> 13.2	> 12.4		> 11.3	

well determined physical parameters of components of eclipsing binaries. For the lower masses of interest in this paper, the use of detailed model atmospheres and an explicit treatment of radiative transfer at the surface are major factors in producing realistic results. At the present time, Burrows et al. 1997 and Baraffe et al. 1997 provide the most adequate treatment of the atmosphere boundary condition, using the new, still unpublished Allard NextGen models. The differences between these two sets in this range are minor; we have used the tracks of Burrows et al. 1997 in the analysis presented here.

3.3. Modeling the infrared excess

The spectral energy distributions of sources with infrared excesses are approximated as described by CRBR, based on the circumstellar envelope models of Adams et al. 1987. The amount of infrared excess required is parametrized by the spectral index $n = d\log(\lambda f_\lambda)/d\log\lambda$: a stellar photosphere radiating like a blackbody would have $n = -3$, and $n > -3$ implies infrared excess. The results of this approximation reproduce well both the observed T Tauri locus and the model predictions of Lada & Adams 1992 (which are also based on the work of Adams et al. 1987). They also agree over the wavelengths sampled by our observations with the model spectral energy distributions of stars surrounded by disks or infalling envelopes calculated by Calvet et al. 1997 and Meyer et al. 1997. Temperature-dependent photospheric features have been computed using the synthetic spectra of cool photospheres of Allard & Hauschildt 1995.

3.4. Foreground extinction

The adopted extinction law is that of Rieke & Lebofsky 1985 for wavelengths below 4.5 μm. Deviations from a universal extinction law in star forming regions such as ρ Ophiuchi are well known (Mathis 1990), but they seem to affect mostly wavelengths shorter than those used in our analysis. In the JHK bands, the detailed analysis of the extinction in ρ Ophiuchi of Kenyon et al. 1998 confirms the applicability of the results of Rieke & Lebofsky 1985. For longer wavelengths, the analysis of line ratios in the direction of the galactic center carried out by Lutz et al. 1996 using ISO SWS data give an extinction at 4.5 μm similar to the one derived by Rieke & Lebofsky, but the values found around 6 μm by Lutz et al. are larger than those that one gets by interpolating the results of Rieke & Lebofsky at that wavelength. We have adopted Lutz et al.'s extinction law for the ISOCAM passbands. However, for the levels of obscuration of our targets (see Sect. 4), the relative transparency of the dust near 6 μm makes the uncertainties due to the choice of the extinction law of the same order as the uncertainties in the photometry.

3.5. Effects of binarity

Some of the objects in our sample may be unresolved binaries, as can be expected given the large fraction of binaries detected among T Tauri stars (Brandner et al. 1996). Undetected binarity in this mass range can affect our fits in different ways, depending on the mass ratio of the system. If one of the components is cooler than the other, the combined spectral energy distribution of the system is dominated by the brighter member in the near infrared, with the fainter and cooler companion contributing at longer wavelengths. The effect of the companion would then be similar to that of a circumstellar excess, and the parameters of the primary will be well estimated by our method. If the system has two components of similar brightness and temperature, the isochrone fitting will yield a single object with higher temperature, extinction, luminosity, and mass than those of each component. Binarity can thus lead us to classify a brown dwarf erroneously as a star, but not the opposite.

4. Results

A summary of the best fitting parameters for each source is given in Table 5. The quality of the fit was estimated from the average of the quadratic sum of the residuals, most of them weighted with the inverse of the estimated error in magnitude. We gave

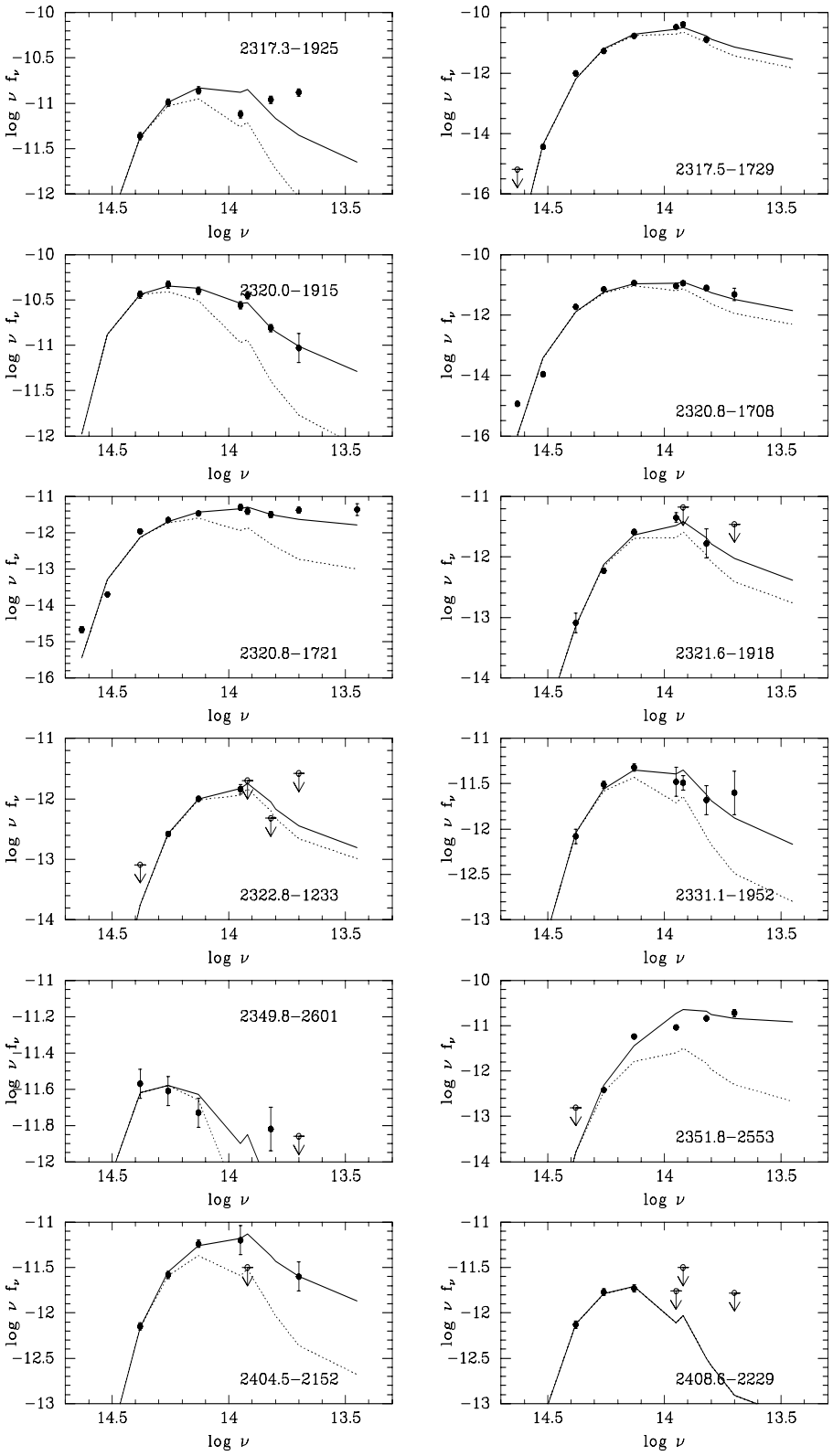

Fig. 1. Best fits to the available photometry. The solid line is the fitted spectral energy distribution of a star surrounded by circumstellar material, obscured by foreground extinction. The dotted line is the intrinsic spectral energy distribution of the star without the circumstellar excess, obscured by the same amount of foreground extinction. The frequency is given in Hz, and νf_ν in erg s^{-1} cm^{-2}

only half of this weight to the residuals in R and I, because the combination of the cool temperatures of our objects and the strong extinction cause large flux gradients in this region, and the effective extinction over the filter width thus becomes a complicated function of the spectral energy distribution of the source and the transmission curve of the filter. A smaller weight was also given to the measurements longwards from SW1, due to the fact that our modeling of the intrinsic infrared excess

Table 5. Best fitting parameters to the available photometry

Object	A_V	n	age	T (K)	M ($M_\odot$)
2317.3-1925	9	-2.2	young	2850	0.07
2317.5-1729	25	-2.7	young	3050	0.23
2320.0-1915	2	-2.1	young	2850	0.08
2320.8-1708	18	-2.9	old	3150	0.20
2320.8-1721	10	-1.6	old	2650	0.04
2321.6-1918	24	-2.6	old	2850	0.07
2322.8-1233	28	-2.8	young	2750	0.05
2331.1-1952	11	-2.3	young	2650	0.04
2349.8-2601	0	-2.1	old	2450	0.02
2351.8-2553	45	-1.1	young	2900	0.09
2404.5-2152	14	-2.1	young	2750	0.05
2408.6-2229	8	-3.0	old	2550	0.03

probably gives only a rough approximation to the true spectral energy distribution in the disk emission-dominated region

In Table 5, we give for each object the visual extinction A_V (assuming $A_V = 8.93 A_K$; Rieke & Lebofsky 1985), spectral index n, temperature T, and mass M. Also indicated is whether an "old" or a "young" isochrone provide the best fit, where the separation between these cases is set at $2 \cdot 10^6$ years. This age is about half of the estimated age of the ρ Ophiuchi complex given by Wilking et al. 1989, which is roughly consistent with that estimated by Comerón et al. 1996 in their reanalysis of the CRBR data. Although the isochrones considered were spaced by intervals of $5 \cdot 10^5$ years, the quality of the fits was insensitive to changes between consecutive isochrones; therefore, we feel that it is not meaningful to give more precise values of the best fitting age. The mass given by the fit, on the contrary, does have some sensitivity to the chosen isochrone, especially at the earliest evolutionary stages, and choice of one or another particular isochrone within the same age group may occasionally move a star from the brown dwarf to the stellar domain or vice versa. The masses listed in Table 5 correspond to ages of 10^6 years for the young group, and $3 \cdot 10^6$ years in the old group. In some cases for which the quality of the fit is similar for ages in the "young" or the "old" range, it has been possible to make a choice based on spectra obtained by Williams et al. 1995 and, more recently, by Meyer et al. 1998. Such cases are noted in the discussion of individual objects below.

The best fitting spectral energy distributions given by the models for the objects listed in Table 5 are illustrated in Fig. 1. Also plotted are the contributions of the stellar photosphere without circumstellar excess in the cases when such excess is required to obtain a good fit.

The required circumstellar excess is fairly insensitive to the chosen isochrone over the whole range of ages considered here. However, even moderate deviations (by a few tenths) in the slope of the excess, n, from the values quoted in Table 5 produce clear departures from the observed fluxes at the longest wavelengths. These deviations cannot be removed by varying the level of foreground extinction or the temperature of the central object. The constraints on n are particularly strong for the objects detected at LW1 or LW4, which stresses the importance

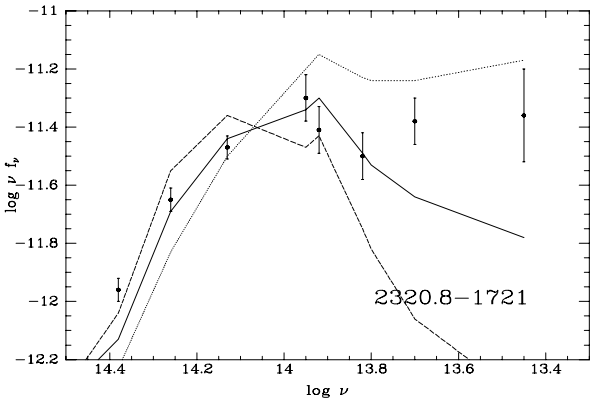

Fig. 2. Comparison between fits to the observed spectral energy distribution of source 2320.8-1721. The solid line corresponds to the best fitting value $n = -1.6$, the dashed line to $n = -2.6$, and the dotted line to $n = -0.6$. To expand the vertical scale so that the differences can be clearly seen, the two data points in R and I have been left out of the plot.

of the good spectral coverage provided by ISO in improving the object/excess/extinction decomposition. To illustrate this point, Fig. 2 shows the best fits to 2320.8-1721 at wavelengths longer than 1.25 μm obtained by imposing three different values of the spectral index: $n = -1.6$ (the best fitting one; solid line), $n = -0.6$ (dotted line), and $n = -2.6$ (dashed line). In each case the extinction and photospheric temperature have been optimized. It is clear that only $n = -1.6$ produces an acceptable fit to the shortest and the longest wavelengths simultaneously, even if the fluxes longward from LW1 suggest that more excess may be required to fit this region. However, a better model fit at long wavelengths would produce discrepances exceeding a factor of 2 in the photosphere-dominated near infrared, where the JHK fluxes are generally measured with a greater accuracy and the spectral energy distribution modeling is much more reliable. Our fits give more weight to the short wavelength measurements, as explained above; departures at the longer wavelengths are most probably due to our simplified way of modeling the excess of circumstellar origin, coupled with the smaller photometric accuracy.

4.1. Discussion of individual objects

2317.3-1925

The fit implies a mass $M = 0.07\,M_\odot$ for an age of 10^6 years and close to the stellar/substellar borderline for any age within the range expected for Ophiuchus sources. The inferred temperature, around 2850 K, varies little with the chosen isochrone. The spectrum of this object presented by Williams et al. 1995 led them to place the temperature slightly below 3000K, in agreement with the uncertainties of our fit. More recent K-band spectra lead Meyer et al. 1998 to assign a M7.5 spectral type to this object. We can consider therefore that all these results are in good agreement.

The ISOCAM measurements are poorly fitted[1], but the detection at LW1 and LW4 suggest a cold infrared excess. In fact, the large LW4 flux suggests a spectral index shallower (i.e., with a smaller absolute value) than -2.2 which, if extrapolated to shorter wavelengths, would imply a smaller photospheric contribution at K and an accordingly lower mass and luminosity.

The JHK photometry of CRBR and that obtained by Strom et al. 1995 agree to better than 0.05 mag in each filter, indicating the source is not strongly variable.

2317.5-1729

The fit is nearly insensitive to the age over the considered range, and indicates a mass in the interval 0.20 - 0.24 $M_\odot$, with almost no circumstellar excess. This mass is in agreement with the rather early spectral type M5 found by Meyer et al.1998. The new infrared observations from La Silla in April 1997 suggest that this object may be now somewhat bluer than at the time of the observations reported by CRBR: the K magnitude is approximately the same, but the source is brighter by about 0.4 and 0.3 mag in J and H, respectively. Other objects in the same frame (2320.8-1708 and 2320.8-1721) do not show such a difference. This source was also detected at I with the NTT. The I magnitude is in good agreement with the extrapolation of the CRBR + ISO fluxes from longer wavelengths, but falls somewhat low if the most recent JHK values are used. A trend for I to fall below the best fitting spectral energy distribution is also observed in the other two sources observed in this band.

2320.0-1915 = GY5

This object appears to be a low mass star or massive brown dwarf with a moderate excess and light extinction. Fits to the photometry do not allow a clear choice between a young or an old age. A temperature of $\simeq 2850$ K provides a good fit if the object has an age of 10^6 years. The 2 μm spectrum indicates a temperature slightly above 3000K (Williams et al. 1995; Meyer et al. 1998 classify it as M7), still consistent with our fit but perhaps indicating that a somewhat older isochrone could be more appropriate; in that case, the mass would be around 0.10 $M_\odot$. An alternative explanation may be the veiling of spectral features by circumstellar emission, as suggested by the infrared excess derived from ISOCAM observations. The photometry is in agreement with that of Strom et al. 1995, but our J is brighter than that of Greene & Young 1992 by 0.48 magnitudes, out of the quoted uncertainties. However, our K magnitude agrees with that of Greene & Young.

[1] It was not possible to measure the SW1 flux for this object due to its proximity to a dead pixel in the SW detector, which caused occasional problems with the Saclay transient model fitting (see Appendix A). However, a comparison with the image of source 2320.0-1915 in the SW1 frame uncorrected for the transient behaviour of the detector suggests that the flux of 2317.3-1925 in this band is similar to that in L'.

2320.8-1708 = GY10

Best fits are obtained with masses between 0.1 and 0.2 $M_\odot$, depending on the age; a wide range of ages provides similarly acceptable fits. The residuals are slightly better assuming an old age, but the spectral features (Williams et al. 1995) tend to favour a temperature, and hence an age and mass, on the lower side. This is confirmed by the very late spectral type, M8.5, estimated by Meyer et al. 1998. Agreement between these works and our fits is found if the age is around 10^6 years, as in that case our best fit is obtained for a temperature of 2900 K. Overall, the photometry produces a good fit with nearly no circumstellar excess. This object was detected at 1.3 mm by André & Montmerle 1994, with a flux of 75 mJy which may imply the existence of a reservoir of cold dust in its vicinity. Possible variability is suggested by the differences of 0.2 magnitudes in all bands between our JHK photometry and that obtained by Strom et al. 1995. The values listed in Table 3 for this object are in better agreement with those of Greene & Young 1992, but the photometric accuracy of that work is lower. Our new observations carried out in April 1997 yield magnitudes equal, within errors, to those of CRBR.

2320.8-1721 = GY11

The likely substellar nature of this object, already pointed out by Rieke & Rieke 1990, is supported by the new ISOCAM observations. A detailed discussion and spectroscopic observations of 2320.8-1721 in the 2 μm band can be found in Williams et al. 1995. Our fitted temperature is in good agreement with theirs. This object has been also observed by Meyer et al. 1998, who classify it as M6.5. Although Williams et al. 1995 suggested possible variability, based on the differences in equivalent width of the overlying extended H_2 emission, the JHK photometry of CRBR agrees with that of Greene & Young 1992, Strom et al. 1995, and with the new photometry obtained by us in April 1997.

Our best fit is obtained with a moderate age ($3{\cdot}10^6$ years) and a spectral index $n = -1.6$, yielding $M = 0.04$ $M_\odot$. The slow early evolution of objects with such a mass makes this fit nearly mass-independent within the range of ages considered here. A fit implying a mass greater than 0.08 $M_\odot$ would be possible only by assuming an age greater than 10^7 years, which seems to be ruled out by the estimated age of the ρ Ophiuchi complex (de Geus 1992). For this source, such an age is particularly unlikely because of the well-determined infrared excess (see Fig. 1), which would be expected to be uncommon in objects older than $\sim 10^7$ years. Moreover, a fit with an age in excess of 10^7 years would require a temperature above 3000 K, in disagreement with the feature strengths in the 2 μm spectrum.

Despite its youth and the evidence for circumstellar matter around it, the possibility of further accretion raising the mass of this object much above its present value seems very unlikely in view of its non-detection at 1.3 mm by André & Montmerle 1994.

2321.6-1918

The photometry of this object listed in Table 3 can be fitted fairly well by a massive brown dwarf of 0.07 $M_\odot$ with a moderate circumstellar excess. Slightly better fits are obtained for an old age, but the improvement in the quality of the fits is only marginal. The best fitting mass remains substellar for ages below $5{\cdot}10^6$ years, although due to its proximity to the stellar/substellar boundary the brown dwarf character remains doubtful.

An intriguing aspect of this object is the large discrepancy in the measured values of H between CRBR and Strom et al. 1995, amounting to 1.15 magnitudes; however, the difference in K is only 0.27 magnitudes, in agreement within the uncertainties. Follow-up observations should be carried out to confirm such apparent extreme variations in color.

2322.6-1233

The non-detections of this object at SW1, LW4, and, especially, at LW1 rule out a significant circumstellar excess. The mild excess adopted here, $n = -2.8$, maximizes the contribution to the near infrared fluxes by the central source, therefore giving an upper limit to the mass of 0.05 - 0.06 $M_\odot$ for ages between 10^6 and $5 \cdot 10^6$ years. The object is thus another possible brown dwarf.

2331.1-1952 = GY64

The ground-based and ISOCAM photometry for this object is very similar to that of 2320.8-1721, with 2331.1-1952 being only a little brighter at short wavelengths (except perhaps for J, where the CRBR measurement is rather uncertain) and fainter at longer wavelengths. For this reason, a similar fit with a somewhat decreased circumstellar excess produces good results for 2331.1-1952 too, implying that it is also a good brown dwarf candidate. The best fitting mass, 0.05 $M_\odot$, goes over the substellar limit only if the age is of order 10^7 years or more.

This object is promising for further spectroscopic followup. It is only moderately obscured, like 2320.8-1721, making it a promising target for follow-up spectroscopic observations in the visible. At longer wavelengths, on the other hand, the small intrinsic infrared excess should decrease the importance of veiling which otherwise complicates the interpretation of spectra in the 2 μm region (Luhman & Rieke 1998). Its spectrum in this region has been recently obtained by Meyer et al. 1998, and the spectral type M8.5 derived by these authors strongly support the brown dwarf character.

2349.8-2601 = GY141

Rieke & Rieke 1990 and CRBR classified this object as a likely foreground M dwarf, based on its blue colors. Its detection at 4.5 μm by ISOCAM is therefore surprising. However, Luhman, Liebert, & Rieke (1997) have found it to have strong Hα emission and photospheric absorptions that include both giant and dwarf characteristics, indicative of a lower surface gravity than that of an evolved foreground dwarf. The object therefore appears to be a member of the ρ Ophiuchi star forming cluster, but one which has escaped in our direction from the molecular cloud.

A considerable infrared excess, $n = -2.1$, is required to produce an overall fit to the available photometry, although with rather large residuals over the JHK bands. The non-detection at LW4 is still consistent with such an excess. The temperature derived from the fit, 2450K, compares well with that measured spectroscopically by Luhman et al. (1997), 2700 $\pm$ 150K. The fitted mass is $M \leq 0.03\,M_\odot$ for an age below 10^7 years, again in reasonably good agreement with the estimate of 0.045 $\pm$ 0.015 $M_\odot$ derived by Luhman et al. (1997) by placing the object on the HR diagram and using the Burrows tracks as we have.

2351.8-2553 = GY146

No good quality fits to the observed fluxes of this object are possible using tracks for low mass stars. The very red $(H-K)$ is suggestive of a background source or an intermediate-mass star located at the opposite edge of the cloud. CRBR tentatively classified it as a possible Class I source, but weak fluxes at the ISOCAM wavelengths argue against that interpretation.

2404.5-2152 = GY202

A fit can be obtained with any isochrone in the age range of ρ Ophiuchi objects and with a moderate excess. However, the non-detection in SW1 (consistent with the large uncertainty in the L' measurement) is rather puzzling, and might be indicative of strong water absorption. Otherwise, the characteristics of this source are similar to those of 2331.1-1952. In addition, 2404.5-2152 was observed by Williams et al. 1995, who favoured a temperature slightly below 3000K from the strength of the features identified in the 2 μm spectrum, and by Meyer et al. 1998, who confirmed such a low temperature, classifying its spectrum as M7. Our best fitting temperature of 2750 K is in good agreement with the spectroscopic observations, and discards possible fits with masses above 0.08 $M_\odot$, which would require ages above $5 \cdot 10^6$ years and temperatures over 3000 K. All this makes 2404.5-2152 an excellent candidate to be a brown dwarf, although it would be a relatively massive one.

2408.6-2229 = GY218

This faint object has not been detected in L', SW1, or LW4, suggesting its spectral index is not far from $n = -3$. The fit, to JHK photometry alone, gives a mass of 0.03 $M_\odot$, independent of the age over the range from 2.5 to $10 \cdot 10^6$ years. Even smaller masses are derived for ages under $2.5 \cdot 10^6$ years, with similar residuals to the fit. The low fluxes and blue color suggest that this object may be the least massive of our sample, with the possible exception of 2349.8-2601.

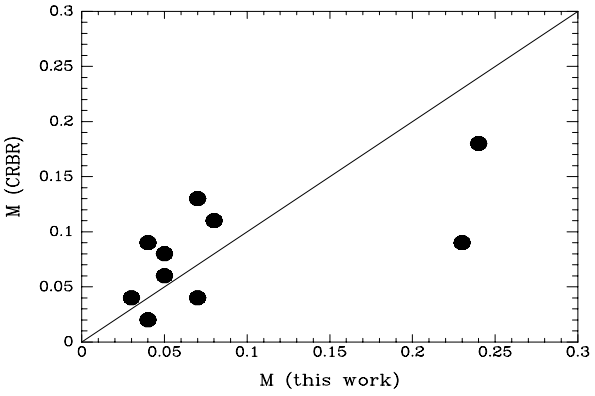

Fig. 3. Comparison between the masses listed in Table 5 and those derived for the same objects by Comerón et al. 1993. Units are in solar masses. Two objects have been excluded from this sample: 2349.8-2601, considered as a probable foreground M dwarf by CRBR, and 2351.8-2553, which CRBR considered a possible Class I object and may be a background source.

4.2. Comparison with other work

The well-constrained fits made possible by combining groundbased and ISOCAM photometry make it of interest to compare the temperatures derived by isochrone fitting with spectral determinations. Details are given in the discussion of individual sources. Of seven objects measured with both techniques, extending from 0.2 $M_\odot$ down to 0.03 $M_\odot$, excellent agreement is achieved in *all* cases. In addition, although all differences are within the expected errors, there is also no discernible trend – that is, the residuals show no bias toward high or low temperatures from the fitting technique compared with spectroscopy. A noteworthy comparison is 2349.8-2601, whose optical spectrum is analyzed in detail by Luhman et al. (1997). Both the temperature and the substellar mass they derive agree with our values from isochrone fitting.

Given the good agreement between spectroscopy and the broadband fits, we can test the quality of the fits based on groundbased infrared photometry alone. Fig. 4 compares the masses derived for the objects studied here with those of CRBR. A good overall agreement exists, despite the more limited wavelength coverage of CRBR and their use of older models of stellar interiors and atmospheres. The only object for which the mass estimate is significantly changed is 2317.5-1729, for which CRBR assumed a strong circumstellar excess unconfirmed by the ISOCAM observations in LW1 and LW4 (see discussion above). The present results thus support the usefulness of fits to ground-based $JHKL'$ photometry, or even JHK only, to study the mass function of embedded populations. At the same time, confirmation of the substellar nature of objects with masses suspected to be near the brown dwarf limit but with strong excesses appears to require observations over a wide range of wavelengths (or spectroscopy).

In the alternate method of Strom et al. (1995), the JHK color-color diagram is used to deredden the sources and estimate their J luminosities, which are finally compared with the theoretical isochrones to obtain masses. The results have been compared with those of CRBR by Williams et al. (1995). The agreement between the two approaches is very good. Thus, the validity of their method is also supported by the ISOCAM observations and analysis.

5. Conclusions

We have used ISOCAM photometry to obtain mid infrared photometry of a sample of low mass embedded objects in ρ Ophiuchi. Combining these data with near infrared groundbased measurements provides strong constraints on models of these sources. We use a technique which simultaneously fits to the extinction, infrared excess, luminosity, and temperature of the object to derive the intrinsic properties of these sources.

Seven of these sources have spectroscopically determined temperatures. The values derived from our fitting are in all seven cases in good agreement. We conclude that the isochrone fitting technique can reliably estimate the source properties when data over the full spectral range of 1 to 6μm are available. We also show that similar modeling based on groundbased data alone (CRBR, Strom et al. 1995) can generally yield reasonably good estimates of the source parameters. Thus, for statistical evaluation of large samples of objects, modeling of groundbased photometry should be valid. However, the example of 2317.5-1729 (whose mass appears to be significantly underestimated from the groundbased data) is a caution about relying on such data for individual objects.

Based on the fits to the photometry, three of the sources in our sample are low mass brown dwarfs (of which two have spectroscopically determined temperatures in agreement with this designation). Five sources are transitional objects, either high mass brown dwarfs or very low mass stars. Three objects appear to be unequivocally young stars. Although the sample was selected to favor previously identified brown dwarf candidates, the results of our new analysis favor our previous arguments (CRBR; Williams et al. 1995; Comerón et al. 1996) that the IMF in ρ Ophiuchi does not drop precipitously at the bottom of the main sequence.

Acknowledgements. We are pleased to acknowledge valuable input on flux calibration from Drs. Joris Blommaert and Alice Quillen. The referee, Dr. Marc Sauvage, is gratefully acknowledged for his careful reading of the first version of the paper and his continued advice on how to improve the data reduction: the paper has greatly benefited from his comments. Dr. Adam Burrows kindly made available to us new evolutionary tracks prior to publication. Dr. Jason Spyromilio is thanked for having allowed us to use part of his service observing time at the NTT. FC wishes to thank the staff of ESTEC and VILSPA for their support during Phase 2 data entry and data reduction, as well as the staff of ESO at La Silla for their assistance during observations. Special thanks go to the astronomer in charge of service observing at the NTT when our observations were done. This work has been supported by Collaborative Research Grants Programme of NATO (CRG 940671), by NASA grants NAGW-4083 and NAG5-3359, and by the CICYT under contract ESP97-1803. The ISOCAM data presented in this paper were analysed using "CIA", a joint development by the ESA

Astrophysics Division and the ISOCAM Consortium led by the ISOCAM PI, C. Cesarsky, Direction des Sciences de la Matiere, C.E.A., France.

Appendix A: instrumental setup and data reduction

ISOCAM observations were obtained using the 3" pixel scale in the microscanning mode, in which frames are obtained by shifting and adding images taken on slightly different positions on the sky. The microscan rasters had 3×3 points, with a step of 3" between each consecutive pair of points. In turn, the images obtained at each raster position were the coaddition of a number of individual short exposures: in this way, basic parameters defining an observation are the integration time of each individual exposure and the number of exposures at each raster point. These parameters were adjusted for each field and filter separately, taking as a reference the expected flux of the faintest sources of interest in each frame, extrapolated by means of a fit to the measured ground-based fluxes at shorter wavelengths. The background sky level at each filter was roughly estimated by using the flux per unit column density and per unit solid angle integrated in the interval from 2 to 15 μm in ρ Ophiuchi, as derived by Boulanger & Pérault 1988. Hydrogen column densities were taken from Loren 1989. Then, the spectral energy distribution of interstellar emission found by Sellgren et al. 1985 for NGC 2023 was upscaled to the expected ρ Ophiuchi values by multiplying by the ratio of estimated integrated fluxes between both regions.

The combination of exposure times and frames per microscan position required to reach a given signal-to-noise ratio was chosen based on the output of the ISOCAM Time Estimator available at the ISO Proposal Data Entry Center in ESTEC. In many cases, the minimum required on-target times for a desired signal-to-noise ratio were obtained for a very low number of individual exposures at each raster position, using an accordingly long time per exposure. This would have been likely to result in a relatively large fraction of pixels discarded because of cosmic ray glitches, thus degrading the quality of the final data. To avoid this, we imposed a minimum number of 12 exposures per raster position.

A very important issue in flux-calibrating ISOCAM observations is the stabilization of the detector: the lower the flux step when the illumination of a pixel is changed, the longer its stabilization time becomes. In staring-mode observations, this can be overcome by taking a number of stabilization exposures before the ones to be actually used for flux measurement purposes; the number of such exposures needed to achieve a 90 % of the stabilized count rate in the pixels illuminated by a source is given by the ISOCAM time estimator as well. The situation changes when microscanning is used, as then there is a flux step in the pixels near the source position every time that the telescope moves to a new raster position. Introducing the necessary stabilization frames at the beginning of each raster point would then imply a prohibitive investment of time. Fortunately, the transient behaviour of the ISOCAM arrays is at present well understood and modelable (Abergel et al. 1996), and a number of algorithms have been developed aimed at providing the necessary corrections leading to a correct flux measurement (Siebenmorgen et al. 1996).

We used an independent Astronomical Observation Template (AOT) for each observation at each filter. Given the low fluxes expected for our sources, a large number of stabilization images (calculated using the ISOCAM Time Estimator as mentioned above) with the same integration time as the science images was taken prior to the first exposure on the first raster position. The observations were then reduced using "CIA", the ISOCAM Interactive Analysis software (Delaney et al. 1996). The reduction procedure of each data cube (i.e., the set of individual images for each field and filter) can be outlined as follows (descriptions of the different steps, algorithms and nomenclature can be found in the ISOCAM Data User Manual, Siebenmorgen et al. 1996):

- Slicing of the data cube into its individual images.
- Dark frame subtraction, using the Cal-G dark frame.
- Cosmic ray glitch removal, using the multi-resolution median transform method.
- Stabilization correction, using the Saclay transient model fitting.
- Normalization to unit exposure time.
- Flat field division, using the Cal-G flat field frame.
- Raster reconstruction.

The processed frame obtained in this way was then transformed into a FITS file, with each pixel value given in ADU s^{-1} normalized to unit gain. A gain factor of 2 was used for all the exposures, as recommended in the ISOCAM Users' Manual, and given the low flux levels of our targets. The pixel values were then transformed to flux units by using the ADU-to-mJy conversion factors for each filter given in the ISOCAM user's manual. No correction for deviations from the νf_ν behaviour assumed in the ADU-to-mJy conversion factor were applied, which seems acceptable in view of the spectral energy distributions in the ISOCAM domain presented in Fig. 1.

Digital photometry was finally performed, and magnitudes were derived, in the way described in Sect. 2.2. As a consistency check of the data reduction and analysis procedure, it is worth noting that the agreement between the ground-based L' measurements and the magnitudes derived in the SW1 filter is in general very good.

References

Abergel, A., et al., 1996, A&A, 315, L329.
Adams, F.C., Lada, C.J., Shu, F.H., 1987, ApJ, 312, 788.
Allard, F., Hauschildt, P.H., 1995, ApJ, 445, 433.
André, P., Montmerle, T., 1994, ApJ, 420, 837.
André, P., Deeney, B.D., Phillips, R.B., Lestrade, J.-F., 1992, ApJ, 401, 667.
Baraffe, I., Chabrier, G., Allard, F., Hauschildt, P.H., 1997, in press.
Barsony, M., Burton, M.G., Russell, A.P.G., Carlstrom, J.E., Garden, R., 1989, ApJ, 346, L93.
Boulanger, F., Pérault, M., 1988, ApJ, 330, 964.
Boulanger, F., Beichman, C., Désert, F.X., Helou, G., Pérault, M., Ryter, C., 1988, ApJ, 332, 328.

Bouvier, J., Appenzeller, I., 1992, A&AS, 92, 481.
Brandner, W., Alcalá, J.M., Kunkel, M., Moneti, A., Zinnecker, H., 1996, A&A, 307, 121.
Burrows, A., Hubbard, W.B., Saumon, D., Lunine, J.I., 1993, ApJ, 406, 158.
Burrows, A., et al., 1998, in preparation.
Calvet, N., Hartmann, L., Strom, S.E., 1997, ApJ, 481, 912. 1995, ApJ, 439, 752.
Casanova, S., Montmerle, T., Feigelson, E.D., André, P., 1995, ApJ, 439, 752.
Cesarsky, C.J., et al., 1996, A&A, 351, L32.
Comerón, F., Rieke, G.H., Burrows, A., Rieke, M.J., 1993, ApJ, 416, 185
Comerón, F., Rieke, G.H., Rieke, M.J., 1996, ApJ, 473, 294.
Comerón, F., Claes, P., Rieke, G.H., 1997, The Messenger, 89, 31.
D'Antona, F., Mazzitelli, I., 1994, ApJS, 90, 467.
Delaney, M., et al. 1996, "ISOCAM Interactive Analysis User's Manual", ESA.
de Geus, E.J., 1992, A&A, 262, 258.
Greene, T.P., Lada, C.J., 1996, AJ, 112, 2184.
Greene, T.P., Meyer, M.R., 1995, ApJ, 450, 233.
Greene, T.P., Young, E.T., 1992, ApJ, 395, 516.
Greene, T.P., Wilking, B.A., André, P., Young, E.T., Lada, C.J., 1994, ApJ, 434, 614.
Kenyon, S.J., Lada, E.A., Barsony, M., 1998, AJ, 115, 252.
Lada, E.A., Adams, F.C., 1992, ApJ, 393, 278.
Leous, J.A., Feigelson, E.D., André, P., Montmerle, T., 1991, ApJ, 379, 683.
Loren, R.B., 1989, ApJ, 338, 925.
Luhman, K.L., 1998, in "Brown dwarfs and extrasolar planets", ed. R. Rebolo, ASP Conf. Series, in press.
Luhman, K.L., Rieke, G.H., 1998, ApJ, in press.
Luhman, K.L., Liebert, J., & Rieke, G.H., 1997, ApJ, 489, L165.
Lutz, D., et al., 1996, A&A, 315, L269.
Mathis, J.S., 1990, ARA&A, 28, 37.
Meyer, M.R., Calvet, N., Hillebrand, L.A., 1997, AJ, 114, 288.
Meyer, M.R., Wilking, B.A., Greene, T.P., in preparation.
Mezger, P.G., Sievers, A., Zylka, R., Haslam, C.G.T., Kreysa, E., Lemke, R., 1992, A&A, 265, 743.
Rebolo, R. (ed.), 1998, "Brown dwarfs and extrasolar planets", ASP Conf. Series, in press.
Rieke, G.H., Lebofsky, M.J., 1985, ApJ, 288, 618.
Rieke, G.H., Rieke, M.J., 1990, ApJ, 362, L21.
Rieke, G.H., Ashok, N.M., Boyle, R.P., 1989, ApJ, 339, L71.
Sellgren, K., Allamandola, L.J., Bregman, J.D., Werner, M.W., Wooden, D.H., 1985, ApJ, 299, 416.
Siebenmorgen, R., Starck, J.-L., Cesarsky, D.A., Guest, S., Sauvage, M., 1996, "ISOCAM Data Users Manual", ESA.
Strom, K.M., Kepner, J., Strom, S.E., 1995, ApJ, 438, 813.
Strom, K.M., Strom, S.E., Edwards, S., Cabrit, S., Skrutskie, M.E., 1989, AJ, 97, 1451
Trimble, V., 1995, in "The bottom of the main sequence -and beyond", ed. C. Tinney, Springer-Verlag.
Williams, D.M., Comerón, F., Rieke, G.H., 1995, ApJ, 454, 144.
Wilking, B.A., Lada, C.J., Young, E.T., 1989, ApJ, 340, 823.